Micro-mechanism of fatigue crack growth: comparison between carbon black filled natural and styrene butadiene rubbers

Jean-Benoit Le Cam, Erwan Verron, Bertrand Huneau, Laurent Gornet, F. Perocheau

Micro-mechanism of fatigue crack growth: Comparison between carbon black filled NR and SBR

J.-B. Le Cam, E. Verron, B. Huneau & L. Gornet
Institut de Recherche en Génie Civil et Mécanique, France

F. Pérocheau
Allevard Rejna Autosuspensions, Dovai cedex, France

ABSTRACT: The present paper investigates the fatigue crack growth in both crystallisable and non-crystallisable elastomers under relaxing loading conditions. The study focuses on the determination of the mechanism of fatigue crack growth. For this purpose, an original "micro-cutting" method developed in a previous study for carbon black filled natural rubber (NR) is employed to observe microscopic phenomena involved in the growth of the crack during SEM observations. In crystallisable NR, the cavitation induced by the decohesion between oxides and rubber matrix is the major fatigue damage and it generates heterogeneous deformation and ligaments (more crystallized zones which resist to crack propagation). In carbon black filled styrene butadiene rubber (SBR), cavities containing zinc oxides fail when the crack propagates and the heterogeneous deformation only induces filaments which do not resist to crack propagation. Based on SEM observation, a fatigue crack growth mechanism in non-crystallisable SBR is proposed. Results are compared with those obtained with NR.

1 INTRODUCTION

Most of the studies dealing with fatigue crack propagation in elastomers are based either on purely mechanical theories (Rivlin & Thomas 1953; Gent 1992) or on fractographic analyses of fracture surfaces (Bhowmick & De 1991). In spite of these researches, it is not possible to predict satisfactorily the crack paths because none of them allow to determine physical phenomena involved in fatigue crack propagation. Previous works showed that the observation of stretched crack tips can be an interesting way to investigate (Gent & Pulford 1984; Bascom 1977). Indeed, using an original "micro-cutting" method applied to stretched crack tips, we recently identified microscopic phenomena involved in the growth of the crack in NR during SEM observations (Le Cam et al. 2004).

In the present study, we recall the results obtained for carbon black filled NR and present similar experiments performed for carbon black filled SBR, i.e. a non-crystallisable elastomer. The aim of experiments is firstly to determine if physical phenomena involved in crack propagation are similar for both compounds and secondly to propose and compare the two mechanisms of fatigue crack growth. In the next Section, the experimental protocol is presented and the in-situ "micro-cutting" method is described. Observation results and mechanisms of fatigue crack growth are given in Section 3. Finally, concluding remarks close the paper.

2 EXPERIMENTAL SECTION

2.1 *Material and sample*

In order to compare fatigue crack growth in both SBR and NR, SBR was filled with 34 phr of carbon black, i.e. the same amount of fillers as in NR compound used in our previous study (Le Cam et al. 2004). Table 1 summarizes their chemical composition and Table 2 presents some mechanical characteristics. NR and SBR were respectively cured for 7 min and 5 min, and the

Table 1. Material formulation (phr).

Components	NR	SBR
Rubber	100	100
Zinc oxide	9.85	10
Oil	3	0
Carbon black	34	34
Sulfur	3	3
Stearic acid	3	3
Antioxidant	2	5
Accelerators	4	4.3

Table 2. Mechanical properties.

Properties	NR	SBR
Density	1.13	1.12
Shore A hardness	58	67
Stress at break (Mpa)	22.9	16.5
Elongation at break	635	343

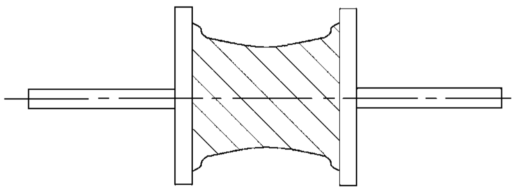

Figure 1. Diabolo sample.

mold temperature was set to 160°C. To overcome aging problems, samples were frozen at −18°, 48 h after their molding. The are thawed out 24 h before testing.

Samples geometry presented in Figure 1 is similar to the one proposed by Beatty (Beatty 1964); it is axisymmetric and is usually called "diabolo sample". Its significant radius of curvature leads to a higher local deformation state in its middle than the enforced nominal deformation. Consequently, the predominant fatigue crack is initiated in the lowest diameter section, i.e. at the center of the sample.

2.2 *Fatigue loading conditions*

In order to generate microstructural fatigue damage in the crack tip vicinity, NR and SBR samples are beforehand tested under uniaxial cyclic enforced displacement conditions. The stretch ratio varies between 1 and 1.33 for the NR compound, and between 1 and 1.5 for the SBR compound. The strain rate was set to limit the rise in temperature of the surface under 20°C, to not superimpose an additional thermal damage to the mechanical damage. In practice, it corresponds to loading frequencies below 5 Hz. These tests are carried out at 23°C regulated temperature until a self-initiated fatigue crack reaches several millimeters long at the surface of the undeformed samples. It takes place at the middle of the sample beside the mould halves joint. Moreover, additional fatigue tests were carried out until fracture in order to connect features of fracture surfaces to crack tips observations.

2.3 *Scanning electron microscopy*

Photomicrographs were performed with a HITACHI S-3200N model SEM using secondary electrons. In order to determine the chemical elements of observed surfaces, an Energy Dispersive Spectrometer of X-rays (EDSX) coupled with the SEM is used. Before observation, elastomer surfaces should be cleaned: here, the specimens are submitted to ultrasounds in a neutral solution. Moreover, as considered materials are not sufficiently conductive, charge-up can locally occur when it is irradiated with the electron beam. Thus, samples can be coated with a 90 nm thick gold layer by vapour deposition to ensure electronic conduction.

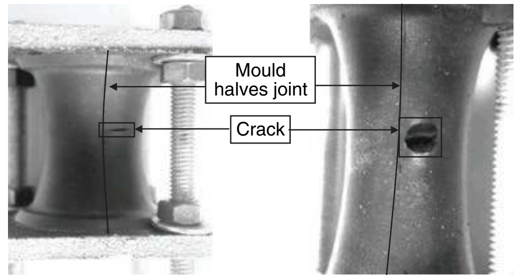

(a) (b)

Figure 2. Tension apparatus.

2.4 *Observation method*

Samples are fixed in a rudimentary static tensile apparatus (see Fig. 2(a)) and they are statically stretched at an elongation equal to 1.67 to open the crack (see Fig. 2(b)). Then, this apparatus is placed in the SEM to observe crack growth. Considering results of Bascom (1977), specimens preparation influence observation results. Indeed, Bascom observed that, in static failure and without coating, the stretched crack tip of nitrile, natural and polybutadiene rubbers have a totally different appearance if observations are performed after that the stretched crack tip was allowed to stand in the laboratory atmosphere about 24 h. In fact, a fibrous and nodular structure appears at crack tip. So long as the specimens were held in the evacuated chamber of the SEM, there was no change in the extent or appearance of the tearing zone. To avoid the effect of ozone attack on the crack tip, Bascom recommends to examine the stretched sample within 0.5 h. Moreover, in this study, it is suspected that the gold layer evaporated on the initial cut gave some protective action against ozone and oxygen attack on rubber. For these reasons, our specimens were observed within 0.5 h after having been stretched, and were retracted after observations. In order to ensure that only fatigue damage is observed, we verify that fibrous and nodular structure does not appear the crack tip. Moreover, we also verify that observations performed with a gold layer the crack tips lead to similar results than those obtained without gold layer.

As mentioned previously, the fatigue test led to initiation and propagation of a crack in the sample, and it involved a fatigue damage in the crack tip vicinity. Thus, the crack tip should be notched to reveal the fatigue damaged zones and to determine their origin. During SEM observations, it is obviously irrelevant to use a laboratory cutting tool to notch the crack. Nevertheless, it is possible to "micro-cut" the crack tip by imparting in-situ a sufficient amount of energy to break cross-links between macromolecules. Two energy sources are used simultaneously: the first one is mechanical and consists in statically stretching samples and the second one consists in locally concentrating the electron beam in the observation zone. In fact, the amount of energy needed to break cross-links cannot easily be determined since the number and nature of cross-links as well as the number of macromolecules in the irradiated zone are not well-known. However, the acquired experience enables us to correctly set the power of the electron beam and to repeat experiments.

3 RESULTS

In this section, results of the microcutting of the SBR crack tip are presented. Then, a mechanism of fatigue crack growth is proposed for non-crystallisable SBR. Finally, this mechanism is compared to the one previously exhibited for NR.

3.1 *Description and comparison of crack tips*

As a summary of our recent study on NR, Figure 3 presents different zones of NR crack tip. It is composed by a few hundred micrometers long ligaments which are highly stretched and surround smooth elliptical surfaces (see Figure 3a). Figure 3b shows the rough surface located at ligaments extremities. It corresponds to retracted broken ligaments. As shown in Figure 3c, zinc oxides which size varies between a few hundred nanometers and 5 μm are embedded in the relief of smooth elliptical areas and can be considered like spherical particles.

Figure 4 presents SBR crack tip which is plane and seems to be exclusively composed by ligaments. They are issued from a linear zone in the middle of the crack also called tear tip by Gent and Pulford during their observations of the crack tip in a precut carbon black filled polybutadiene sample (Gent and Pulford 1984). The fact that crack tip only corresponds to a linear zone in which the crack grows is the first major difference with NR crack tip. In the following, we will use the term tearing line instead of tear line as used by Gent and Pulford. Figure 5 shows zinc oxides between ligaments and the stretched cavity which contained them. As in NR, oxides size varies between a few hundred nanometers and 5 μm. Figure 6 shows

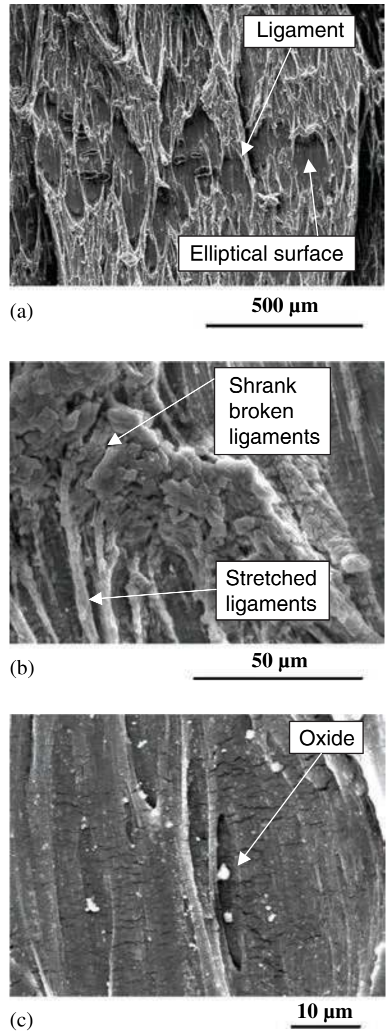

Figure 3. NR crack tip.

the bottom of the crack tip in SBR. It corresponds with ellipsoidal zones which shrunk when the crack grew. Here, these ellipsoidal zones are not similar to those encountered in NR. Their formation process will be discussed next.

3.2 *Crack tip microcutting*

In NR, natural micro-cracks occur in elliptical zones surrounded by highly stretched ligaments. When the electron beam is focused a few seconds beside these micro-cracks, artificial micro-cracks initiate at the beam concentration point and propagate until they are stopped by ligaments. During their propagation, artificial micro-cracks reveal cavities similar to the ones

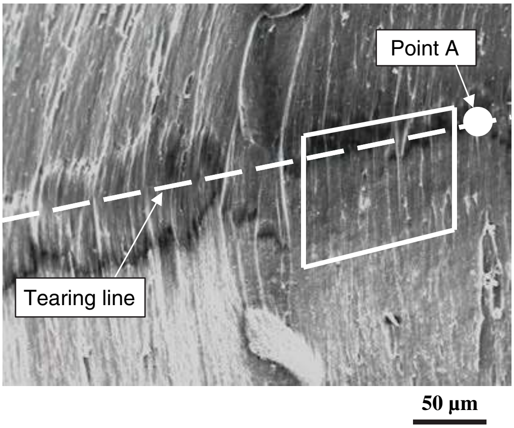

Figure 4. SBR crack tip.

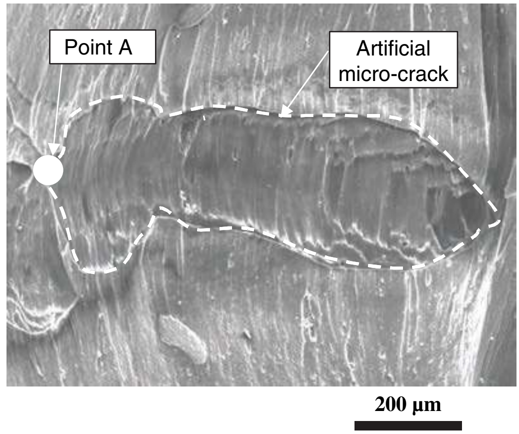

Figure 7. Microcutting at the SBR crack tip.

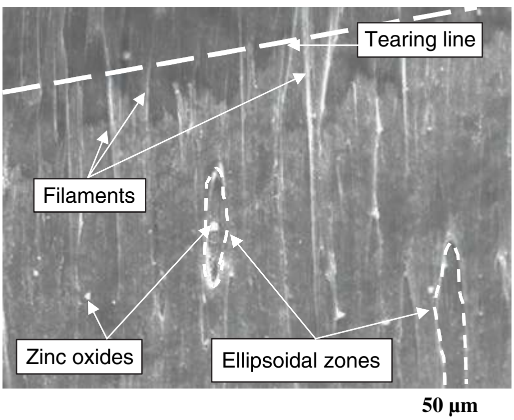

Figure 5. Magnified view of Figure 4.

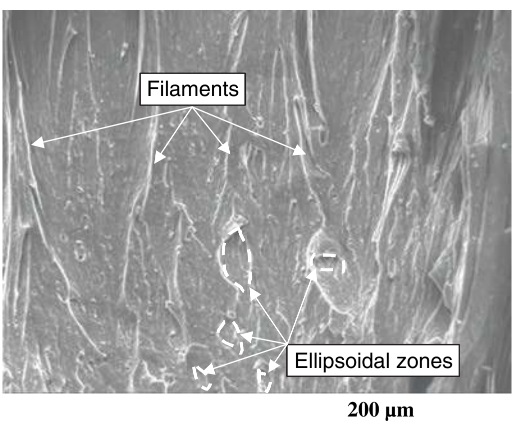

Figure 6. Bottom of crack tip in SBR.

observed in natural micro-cracks. It is notable that if the electron beam is focused on ligaments (the SEM power settings being unchanged), they will not break even if they are exposed for a long time. This experiment highlights that cavities take place in the vicinity of the crack tip due to decohesion between oxides and rubber matrix. They weaken ellipsoidal zones and generate natural micro-cracks. This process leads to the formation of highly stretched and crystallized ligaments. These results obtained under fatigue loading conditions are quiet similar to those recently established under static conditions which demonstrate that a crystallized zone appears at crack tip of initial cut lengths 0.5 and 1 mm for stretch ratios greater than 1 = 1.3 (Trabelsi et al. 2002). Moreover, interesting works has been published on the real-time evolution of crystallization in NR during one loading cycle (Toki et al. 2000).

In SBR, the zone favorable to microcutting obviously corresponds to the tearing line previously described. Thus, the electron beam is concentrated on a point of this tear line (point A in Figure 4). A micro-crack immediately initiates at this point and propagates towards the right side. It is notable that the time needed to initiate micro-crack is very short as compared to the NR case (electron beam energy being identical). Moreover, we observed that the crack growth rate is faster than the NR one. Figure 7 shows the path of this artificial micro-crack. Contrary to NR, ligaments do not stop the artificial micro-crack which breaks them. The fact that ligaments fail under the same energy level than the tearing line is the second major difference with NR. It indicates that SBR microstructure is homogeneous at crack tip and thus in all the sample bulk. In the following, non-crystallized ligaments observed in SBR are called filaments.

Now, it is necessary to determine if these filaments are formed by the same micro-mechanism as ligaments

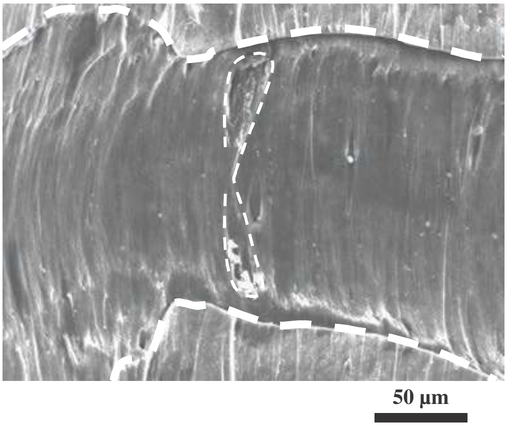

Figure 8. Zoom in encircled zone of Figure 6.

of NR which are issued from the deformation of natural micro-cracks that initiates in the ellipsoidal zones.

We firstly observed the neighborhood of zinc oxides in SBR. Figure 8 shows a magnified view of the encircled zone in Figure 7. It appears that the tip of this artificial micro-crack is similar to the tearing line. The assumption that the microstructure of bulk material is not strain-dependent seems to be relevant. The encircled zone in Figure 8 corresponds to the deformation of a cavity containing zinc oxide particles after being broken by the propagation of artificial micro-crack. If cracking continues in the sample depth, this artificial micro-crack will grow and walls of the cavity are transformed into filaments.

3.3 *Crack growth mechanism*

In NR, results revealed that cavitation induced by the decohesion between zinc oxides and rubber matrix is the major fatigue damage and that the crack tip is composed by stretched elliptical zones surrounded by ligaments. The mechanism of fatigue crack growth suggests that wrenchings located on the fracture surface of NR are formed by the failure of highly stretched ligaments (Le Cam et al. 2004). Moreover, authors explained that ligaments are the most crystallized zones at the crack tip and proposed a mechanism of fatigue crack growth in NR.

Using the previous observations, the mechanism of fatigue crack growth in non crystallisable SBR is proposed in this section. Like the mechanism of fatigue crack growth proposed for NR, chronological sketches describe the phenomenon. Figures 9 presents the front view of crack growth. Here, the mechanism is simpler than that in NR, thus the front view is sufficient to entirely describe the phenomenon.

Figure 9a is a schematic view of the crack tip and more precisely a unit surface of the crack tip. The scale of the description is the one of the encircled zone in Figure 5. As shown in this view which is the first step of crack growth, the crack tip is stretched in the directions of the black arrows on the left and it is composed of filaments and ellipsoidal zones containing zinc oxides (ellipsoidal zones 1 and 2).

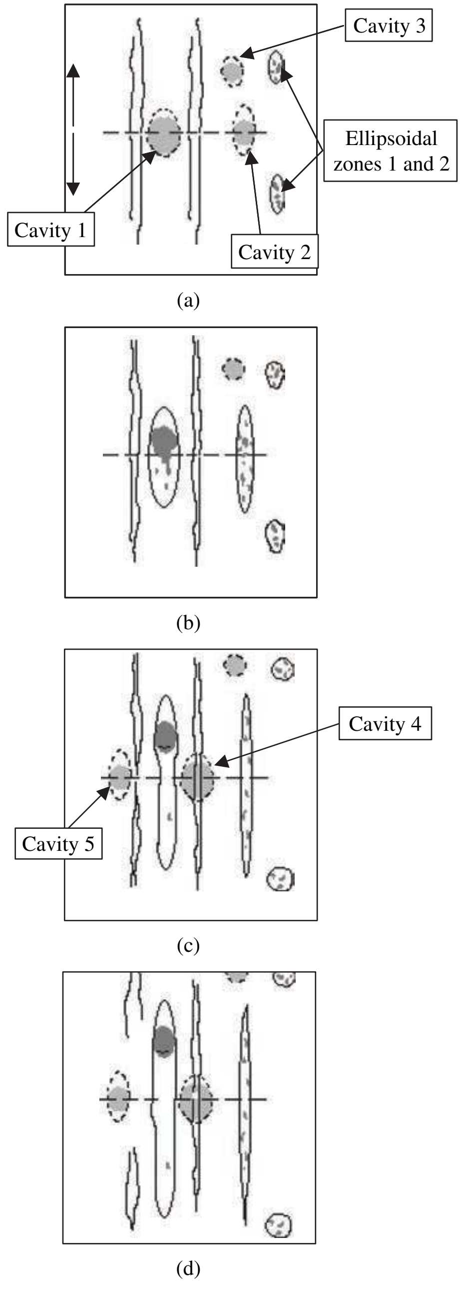

Figure 9. Mechanism of fatigue crack growth in SBR.

Cavities surrounding zinc oxides and hidden in the rubber matrix behind the crack tip appear in dotted lines in this figure (cavities 1, 2, and 3). Their shape is ellipsoidal. Figure 9b presents the second step of crack growth. The crack tip grows on both sides of the tearing line and reveals highly stretched cavities behind it (cavities 1 and 2). Cavities which are not located in front of the tearing line are not revealed (here, cavity 3). During crack growth, ellipsoidal zones 1 and 2 move away from the tearing line, i.e. they are less and less stretched, and their shape become quasi-circular. In the same way, the ellipsoidal shape of cavity 3 become spherical. Figure 9c is the third step of the mechanism and presents the evolution of revealed cavities 1 and 2. It shows that cavities 1 and 2 are more and more stretched and that the crack tip grows towards new hidden cavities (cavities 4 and 5). Highly stretched cavities walls form filaments, i.e. filaments due to the deformation of revealed cavities. Here, we focus on zinc oxides because they are the most numerous particles, but it is notable that these explanations could be applied to inclusions located in rubber matrix, i.e. mineral inclusions which size can reach 300 μm diameter. Figure 9d is the last step of the mechanism. During crack growth, cavity 5 is revealed and grows. Walls of cavities 1 and 2 begin to shrink and form quasi-spherical zones similar to the ones encircled in Figure 6. Finally, the mechanism starts again at the first step of this unit sequence.

4 CONCLUSIONS

As a summary, an original technique of in-situ microcutting allowing to observe crack tips of stretched samples led to propose a fatigue crack growth mechanism. The mechanism in SBR, i.e. non-crystallisable elastomer, is different than the one previously proposed for crystallisable elastomers. Fatigue damage in natural rubber is mostly due to the cavitation induced by the decohesion between oxides and rubber matrix. In SBR, only the failure of cavities containing zinc oxides contributes to the formation of filaments. Filaments are not crystallized since in NR highly stretched ligaments are crystallized and can resist to crack propagation. Moreover, zones in which crack tip propagates correspond to a line in SBR instead of a surface composed of ligaments and ellipsoidal zones in NR. Moreover, we observed that in SBR the amount of carbon black has a significant influence on crack path. Further works will be devote to the influence of the amount and nature of fillers at the microscopic scale.

ACKNOWLEDGMENT

We would like to acknowledge *Allevard Rejna Autosuspensions* for its the financial support and Trelleborg for its collaboration.

REFERENCES

Bascom, W. (1977). Scanning electron microscopy of rubber tear. *Rubber Chem. Technol. 50,* 875–883.

Beatty, J. R. (1964). Fatigue of rubber. *Rubber Chem. Technol. 37,* 1341–1364.

Bhowmick, A. K. & De, S. (1991). *Fractography of Rubber Materials.* London: Elsevier Applied Science.

Gent, A. N. (1992). *Engineering with Rubber.* Munich: Hanser Publishers.

Gent, A. N. & Pulford, C. (1984). Micromechanics of fracture in elastomers. *J. Mater. Sci. 19,* 3612–3619.

Le Cam, J.-B., Huneau, B., Verron, E. & Gornet, L. (2004). Mechanism of fatigue crack growth in carbon black filled natural rubber. *Macromolecules 37,* 5011–5017.

Rivlin, R. S. & Thomas, A. G. (1953). Rupture of rubber. I.Characteristic energy for tearing. *J. Polym. Sci. 10,* 291–318.

Toki, S., Fujimaki, T. & Okuyama, M. (2000). Strain-induced crystallization of natural rubber as detected real-time by wide-angle x-ray diffraction technique. *Polymer 41,* 5423–5429.

Trabelsi, S., Albouy, P.-A. & Rault, J. (2002). Stress-induced crystallization around a crack tip in natural rubber. *Macromolecules 35,* 10054–10061.